Characterization of plasma-sprayed and whisker-reinforced alumina coatings

NOBUYA IWAMOTO, NORIMASA UMESAKI*, SHIGEKI ENDO‡
Welding Research Institute, Osaka University, 11-1, Mihoga-oka, Ibaraki-city, Osaka 567, Japan

TOSHIRO MORIMURA
Ceramics Division, Showa Denko Co. Ltd, 1-13-9, Shiba-daimon, Minato-ku, Tokyo 105, Japan

We have strengthened plasma-sprayed alumina coatings by incorporating SiC or Si_3N_4 whiskers. As a result, we found that the whisker-reinforced coatings were greatly improved in properties such as thermal shock resistance and adhesion. Major features of the plasma-sprayed Al_2O_3–5.0 wt % Si_3N_4 coating were investigated by means of scanning electron microscopy, secondary ion mass spectroscopy, X-ray diffraction, X-ray fluorescence spectroscopy and thermal radiation measurements.

1. Introduction

In the past few years, significant advances have been made in producing fusion conditions in nuclear fusion reactor devices such as tokamak. Nevertheless, the fusion reactor vessel must withstand many adverse conditions such as ion sputtering, arcing, swelling, blistering, contamination of plasma by vaporized metal ions, high temperature fatigue, etc. Therefore, it is recommended that the metal surface of reactor vessel is coated with low atomic number materials. Aluminium oxide is considered to be a candidate insulator for several fusion reactor applications, for example, the current breaker in the tokamak, neutral beam injectors for the tokamak and mirror devices, and direct converters for the mirror device [1]. Plasma spraying is an attractive technique for coating metal surfaces with complex shapes and large area such as the current breaker in the tokamak. Unfortunately, in the case of plasma spraying, it is difficult to obtain strong adhesion between the coating and the metal substrate.

It is well known that fibre reinforcement is effective for improving the mechanical properties of ceramics [2]. The fibres can prevent cracks in ceramics from propagating. Also, there is a stress transfer to the entire composite coating because of strong adhesion between the fibre and the ceramic. Therefore, in order to strengthen plasma coatings, we have developed a manufacturing method for SiC or Si_3N_4 whisker-reinforced alumina coatings. Until now, no reported attempts have been made to produce the whisker-reinforced ceramic coating by plasma spraying.

In this study, we have measured the mechanical properties of plasma-sprayed alumina coatings which were reinforced by SiC or Si_3N_4 whiskers. The Al_2O_3–5.0 wt % Si_3N_4 coating was characterized by means of scanning electron microscope (SEM), secondary ion mass spectroscopy (SIMS), X-ray diffraction (XRD), X-ray fluorescence spectroscopy and thermal radiation measurements.

2. Experimental procedure
2.1. Preparation

Blended powders of alumina (Showa Denko Co. Ltd, Japan) and SiC or Si_3N_4 whiskers (Tateho Chemical Industries Co. Ltd, Japan) were used for plasma spraying. The properties of these materials are given in Table I. Carbon steel (ANSI/ASTM A570-79 Grade 45, size: 50 mm × 50 mm × 6 mm) was used as a substrate metal, and one surface of each steel plate was blasted by alumina sand before plasma spraying. The six alumina ceramic coatings, Al_2O_3, Al_2O_3–1.5 wt % SiC, Al_2O_3–3.0% SiC, Al_2O_3–1.5% Si_3N_4, Al_2O_3–3.0% Si_3N_4 and Al_2O_3–5.0% Si_3N_4, were

TABLE I Material properties

Material (size)	Chemical composition	Morphology
Alumina powder (10 to 44 μm)	Al_2O_3 = 99.8% SiO_2 = 0.03% Fe_2O_3 = 0.02% Na_2O = 0.15%	α-Al_2O_3
SiC whisker (0.05 to 0.2 μm diameter 10 to 44 μm long)	SiC > 98% Mg < 0.25% Ca < 0.38% Al < 0.06% Fe < 0.001%	β-SiC > 95% α-SiC < 5%
Si_3N_4 whisker (0.2 to 0.5 μm diameter 50 to 300 μm long)	Si_3N_4 > 99% Mg < 0.15% Ca < 0.20% Al < 0.12% Fe < 0.1%	α-Si_3N_4 > 97% β-Si_3N_4 < 3%

---

*To whom correspondence should be addressed.
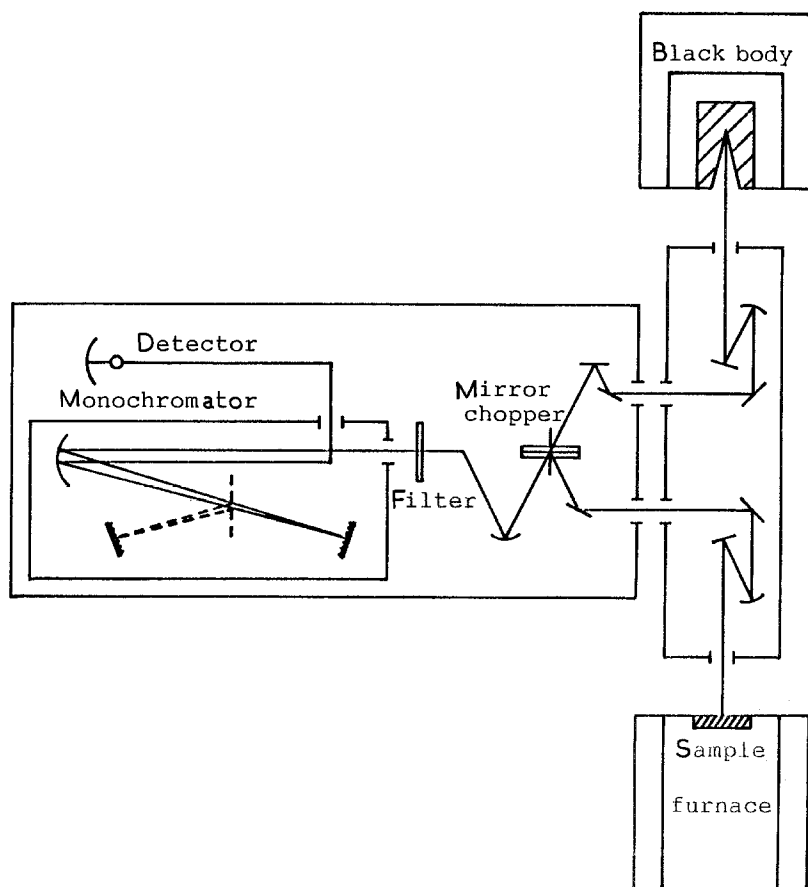‡*Present address*: Bridgestone Co. Ltd, Tokyo, Japan.

1113

Figure 1 Optical system of thermal radiation measurement.

manufactured with the plasma spraying conditions shown in Table II.

2.2. Mechanical tests

Mechanical tests were carried out on Al_2O_3–1.5% SiC, Al_2O_3–3.0% SiC, Al_2O_3–1.5% Si_3N_4 and Al_2O_3–3.0% Si_3N_4 coatings.

The thermal shock resistance of the coated samples was examined during a thermal cycle which consisted of heating for 60 sec at 1373 K with a propane–oxygen burner and then cooling for 60 sec by spraying water at ambient temperature on the back side. The test was terminated when cracking was observed by eye.

The adhesion between alumina coatings and substrates was examined individually by a steel ball–gravity impact test (commonly termed a drop test). At scheduled periods a steel ball weighting 100 g was dropped from a height of 825 mm, and the samples were inspected for the first signs of cracking in the coatings by eye. When cracking of the coatings occurred, the test was terminated.

2.3. Analytical characterization

The SEM-EDX (Jeol, LSM-840) was used at a voltage of 25 kV and current of $1 \times 10^{-9} \mu A$.

TABLE II Plasma-spraying conditions

Equipment	Plasma Technic PT Allgas system
Arc gases	Primary: Ar(35 l min^{-1})
	Secondary: H_2(8 l min^{-1})
Voltage and current	65 V and 750 A
Powder carrier gas	Ar (9 l min^{-1})
Spraying distance	80 mm
Thickness of coatings	150 μm

The SIMS microanalysis was carried out in a Hitachi IMA-SS under a vacuum of 3.0×10^{-3} Pa. The acceleration voltage was fixed at 10 kV, and Ar^+ was used as the primary ion.

X-ray diffraction was performed with the use of a Rigaku θ–θ diffractometer with parafocusing geometry and Cu$K\alpha$ (40 kV and 20 mA) radiation which was monochromatized by a curve graphite monochromator mounted in the diffracted beam. The scanning speed was $1°$ min^{-1}.

The fluorescence X-ray spectra were taken with a Rigaku fluorescence X-ray spectrometer (Model 9578) using a rhodium target. The excitation voltage and current were 40 kV and 40 mA. An EDDT (ethylene diamine D-tartrate, $C_6H_{14}N_2O_6$) crystal was used as an analysing crystal. The step-scanning was made at $\Delta 2\theta$ intervals of $0.02°$ with a counting time of 8 to 80 sec. The centre of the bandwidth at half intensity was taken as the peak position. The peak shifts of the Si$K\beta$ line were measured in comparison with the peak of silicon.

Thermal radiation properties of the coatings were measured by an infrared spectrometer (Jasco, A-302) with the optical system shown in Fig. 1. The normal emissivity spectra in the frequency range from 2 to 30 μm were observed at 895 and 944 K.

3. Results and discussion
3.1. Mechanical properties
Fig. 2 shows the results of the thermal shock test with error limits on the collected data. The addition of SiC or Si_3N_4 whiskers produced an increase in the thermal shock resistance of the coated samples, which increased with increasing whisker content. Crack propagation in
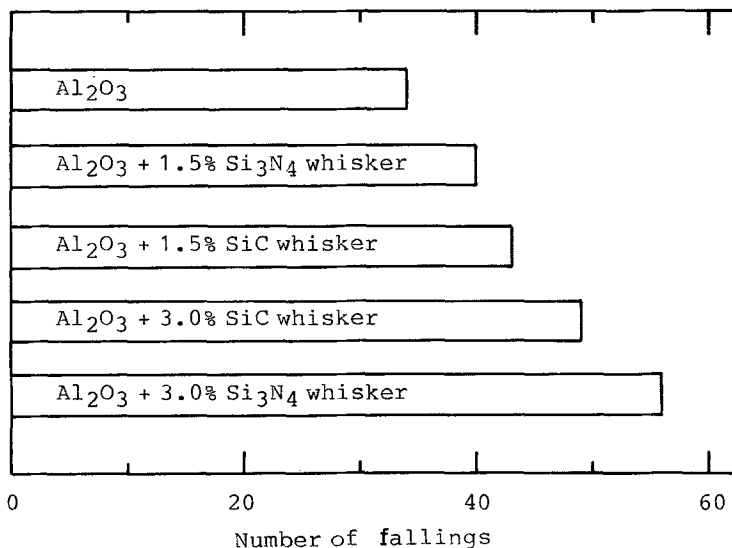
Figure 2 Results of thermal shock test. Two tests were averaged for each point.

Chart bars (Number of fallings):
- Al_2O_3
- Al_2O_3 + 1.5% Si_3N_4 whisker
- Al_2O_3 + 1.5% SiC whisker
- Al_2O_3 + 3.0% SiC whisker
- Al_2O_3 + 3.0% Si_3N_4 whisker

Number of fallings (0, 20, 40, 60)

the coating was impeded by the incorporation of the SiC or Si_3N_4 whiskers, resulting in a toughened whisker–alumina coating system.

In Fig. 3, the data from the drop test shows that the number of impact cycles to failure for the whisker-reinforced alumina coatings increased by 1.5 to 4 times over the alumina coating without whisker, and increased with whisker content.

It is, therefore, concluded that whisker reinforcement significantly improved the mechanical properties, i.e. the thermal shock resistance and impact toughness of the plasma ceramic coating.

3.2. Characterization

The Al_2O_3–3% Si_3N_4 coating showed the best mechanical properties of the five samples, but we characterized only the Al_2O_3–5% Si_3N_4 coating.

The SEM micrographs of the Al_2O_3–5% Si_3N_4 coating and the corresponding X-ray maps for selected elements silicon and aluminium are shown in Figs 4 and 5. The X-ray map in Fig. 4 illustrates that silicon was distributed thoughout the plasma-sprayed alumina coating. As can be seen from Fig. 5, the Si_3N_4 whisker

caught in the alumina coating can be clearly revealed under high magnification.

Fig. 6 shows the SIMS depth profiles of sodium, potassium, calcium and silicon relative to aluminium in the Al_2O_3–5% Si_3N_4 coating. As shown in this figure, the relative intensity ratio Si/Al was almost independent of sputtering time. The results indicate that the silicon nitride phase was uniformly distributed in the Al_2O_3–5% Si_3N_4 coating.

Fig. 7 shows the X-ray diffraction patterns of the Al_2O_3–5% Si_3N_4 before and after plasma spraying. It is well known that there are two polymorphs, α and β, of Si_3N_4. Turkdogan et al. [3] and Forgeng and Decker [4] pointed out that α-Si_3N_4 can transform to β-Si_3N_4 on heat treatment in excess of 1800 K. As shown in Fig. 7, the X-ray diffraction pattern after spraying indicated that the original Si_3N_4 phase remained as α-Si_3N_4 in the alumina coating without α–β phase transformation and no reaction between Si_3N_4 and the Al_2O_3 matrix was observed. It is known that α-Si_3N_4 is a stable compound from the Si–O–N phase diagram [5]. Furthermore, the X-ray diffraction pattern after spraying shows that there was no evidence of sialon
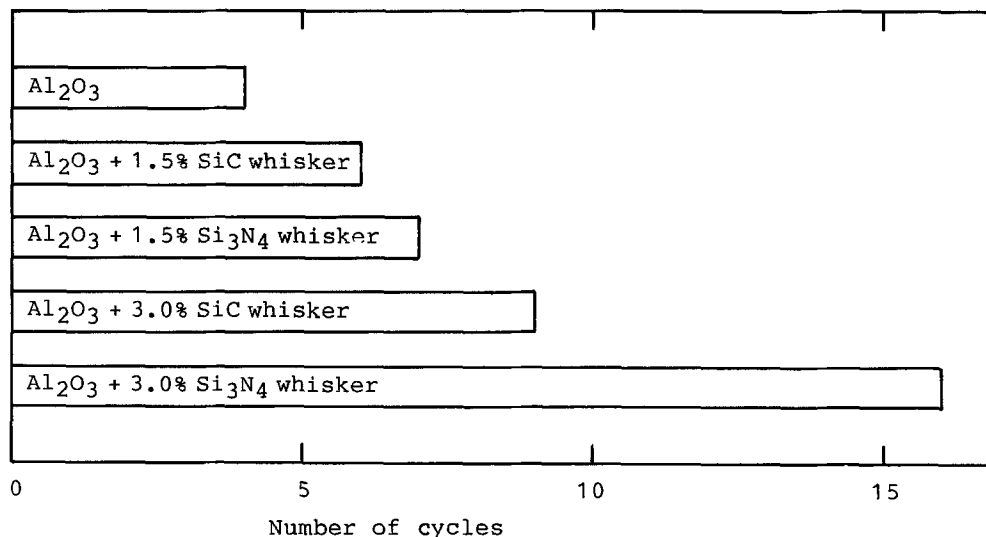

Chart bars (Number of cycles):
- Al_2O_3
- Al_2O_3 + 1.5% SiC whisker
- Al_2O_3 + 1.5% Si_3N_4 whisker
- Al_2O_3 + 3.0% SiC whisker
- Al_2O_3 + 3.0% Si_3N_4 whisker

Number of cycles (0, 5, 10, 15)

Figure 3 Results of drop test. These tests were averaged for each point.
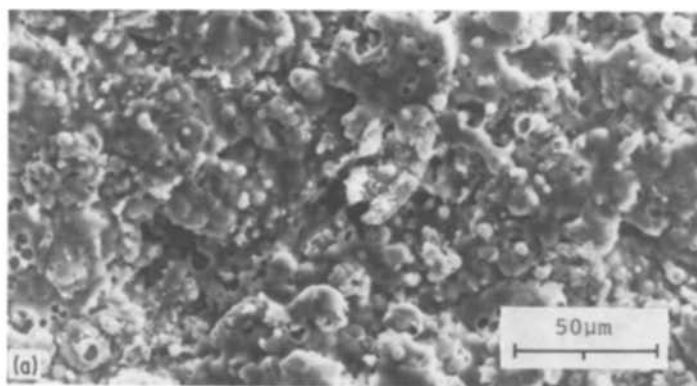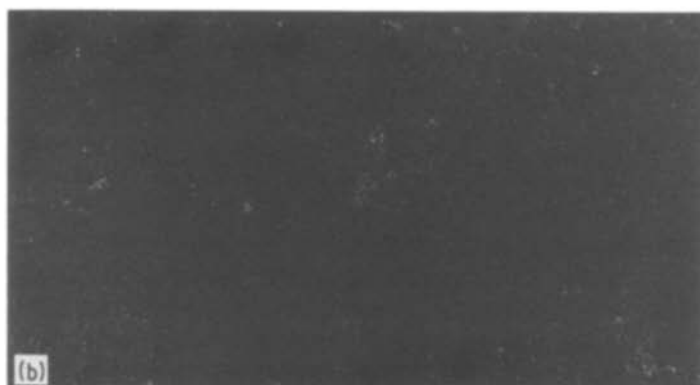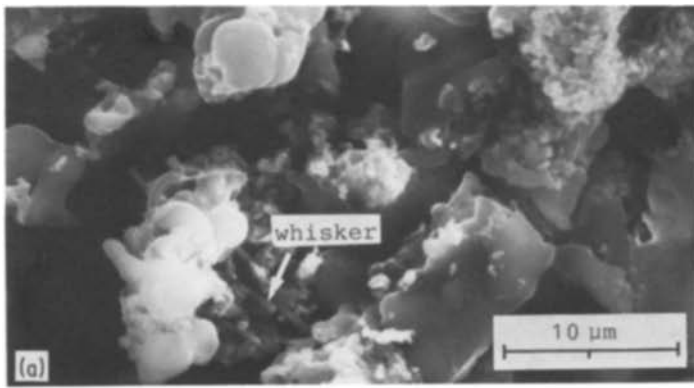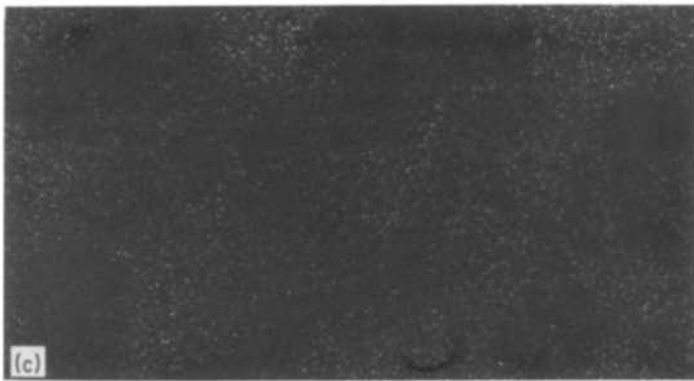
Figure 4 (a) SEM micrograph of plasma-sprayed Al_2O_3–5.0 wt % Si_3N_4 coating and corresponding X-ray map for elements (b) silicon and (c) aluminium.

and silica phases formed by reacting Si_3N_4 whisker and alumina powder together during plasma spraying. In Fig. 7, we also observed seven reflections due to α-Si_3N_4 before spraying, whereas after spraying these reflections were reduced to two, (1 0 1) and (2 0 1), and also the intensity of these reflection peaks decreased. The reason for the change of these reflection peaks before and after spraying is most probably due to the difficulty in feeding powder materials to the plasma-torch, since the Si_3N_4 whiskers are very small.

As can be seen from Fig. 7, when the starting alumina powder consisting of α-Al_2O_3 was plasma-sprayed on a steel substrate, γ-Al_2O_3 was formed, as confirmed by the X-ray data. It is well known that there are several metastable polymorphs such as α-, γ-, η, κ- and θ-Al_2O_3 [6]. Also several metastable polymorphs of alumina are known to form when it is plasma-sprayed on to a cooled substrate [7, 8]. The formation of γ-Al_2O_3 results from quenching the molten alumina spheres. The rapid quenching action, caused by the molten alumina spheres meeting a cold surface, results

in crystallization of γ-Al_2O_3 in preference to α-Al_2O_3 [1, 9].

Dodd and Glen [10] found a well-established relation between the chemical shift of $AlK\beta$ and the coordination number of Al^{3+} ions in oxide crystals. The chemical shift of the silicon peak due to an inner orbital transition, therefore, gives important information concerning the coordination conditions in the Si_3N_4 whisker-reinforced Al_2O_3 coating after spraying.

TABLE III Chemical shift of $SiK\beta$ peak by X-ray fluorescence measurement

Material	$\Delta 2\theta$[EDDT] (deg)	ΔE (eV)	$\Delta\lambda$ (10^{-3} nm)
SiO_2	0.205	2.73	100.7
Si_3N_4 whisker	0.113	1.50	55.2
5.0 wt % Si_3N_4 whisker –Al_2O_3 coating	0.116	1.54	56.7

$\Delta 2\theta = 2\theta$(Si metal)–2θ(sample); $\Delta E = E$(sample)–E(Si metal); $\Delta\lambda = \lambda$(Si metal)–λ(sample).

The values of the chemical shift of $SiK\beta$ for Al_2O_3–5% Si_3N_4 (before and after spraying) and silica, relative to the value of silicon metal and expressed by the angle, energy and wavelength, are summarized in Table III. In contrast to the values of SiO_2, the values for Al_2O_3–5% Si_3N_4 before and after spraying are nearly equal. It can be clearly deduced that the structure of the silicon nitride in the coating is identical to that of the Si_3N_4 whisker before spraying.

Table IV shows the intensity ratios $SiK\alpha/AlK\alpha$ of the Al_2O_3–5% Si_3N_4 before and after spraying. As shown in this table, the ratio $SiK\alpha/AlK\alpha$ after spraying significantly decreased in comparison with that before spraying. This result is in good agreement with the data obtained by X-ray diffraction both before and after spraying. That is, the intensity of the reflection peaks for the α-Si_3N_4 phase after spraying decreased in comparison with that for Si_3N_4 whisker before spraying.

Fig. 8 shows the normal emissivity spectra of Al_2O_3–5% Si_3N_4 coating at 795 and 944 K. From the measurement of normal spectral emissivity $\varepsilon_N(\lambda, T)$, we can calculate the normal total emissivity $\varepsilon_N(T)$ from the following equations:

$$\varepsilon_N(T) = \frac{\int_{\lambda_1}^{\lambda_2} \varepsilon_N(\lambda, T)M_b(\lambda, T) \, d\lambda}{\int_{\lambda_1}^{\lambda_2} M_b(\lambda, T) \, d\lambda} \quad (1)$$

TABLE IV Peak intensity of X-ray fluorescence spectra of Al_2O_3–5.0 wt% Si_3N_4 before and after plasma spraying

Material	$AlK\alpha$ (c.p.s.)	$SiK\alpha$ (c.p.s.)	$SiK\alpha/AlK\alpha$ (%)
Powder material	4870	87	5.44
Sprayed coating	29800	411	1.38

TABLE V Normal total emissivity of plasma-sprayed Al_2O_3–5.0 wt% Si_3N_4 coating

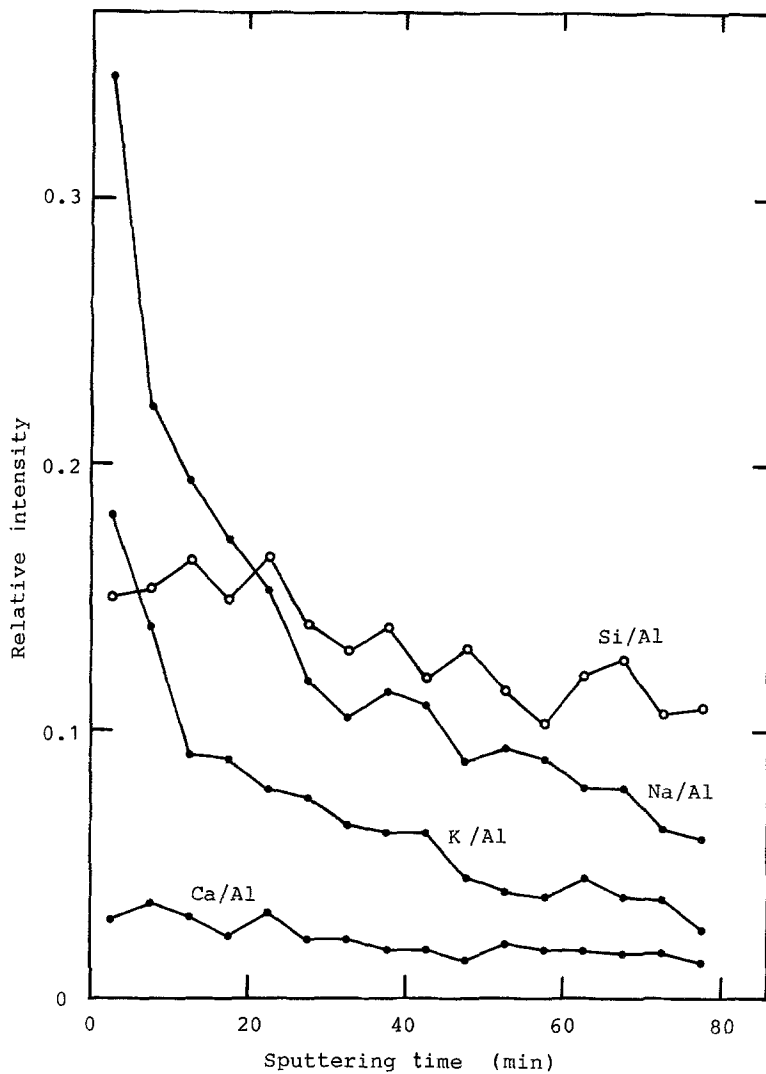| T (K)	λ_1 (μm)	λ_2 (μm)	$\varepsilon_N(T)$
673	3.26	13.90	0.738
873	2.52	10.72	0.591
1073	2.05	8.72	0.481

Figure 6 SIMS intensity ratios, Si/Al, Na/Al, K/Al and Ca/Al of plasma-sprayed Al_2O_3–5.0 wt % Si_3N_4 coating as a function of sputtering time. Si/Al: $I(^{28}Si)/I(^{27}Al)$, Na/Al: $I(^{23}Na)/I(^{27}Al)$, K/Al: $I(^{39}K)/I(^{27}Al)$, Ca/Al: $I(^{40}Ca)/I(^{27}Al)$.
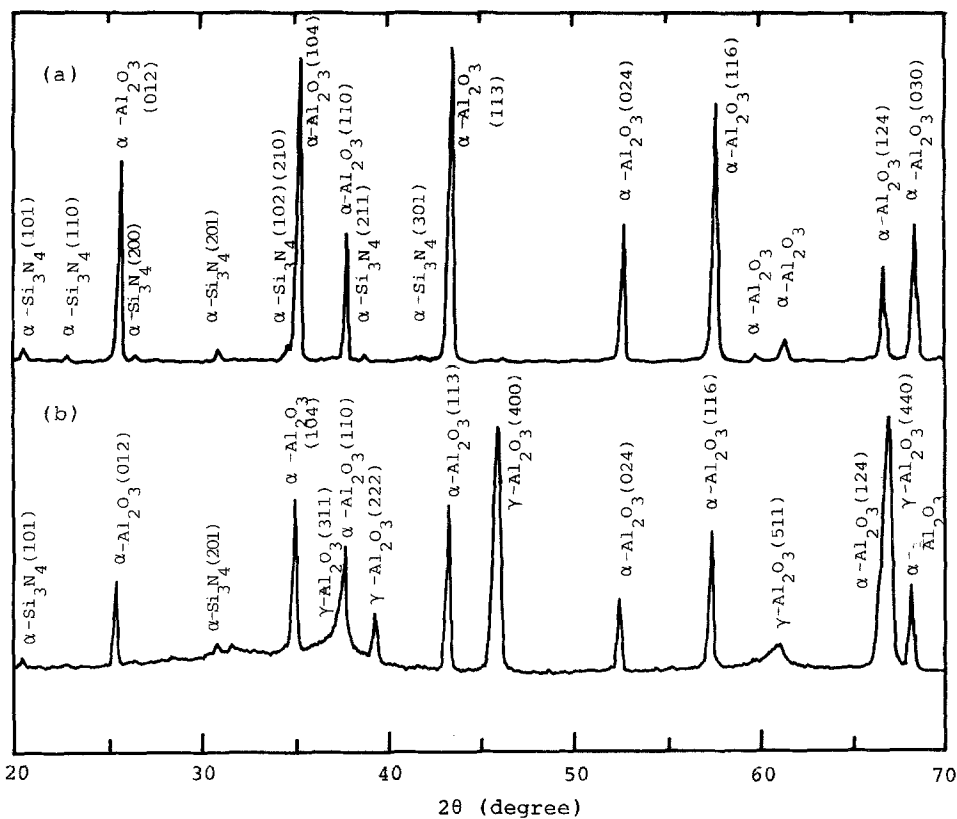
Figure 7 X-ray diffraction patterns of Al_2O_3–5.0 wt % Si_3N_4 before and after plasma spraying (α: α-Al_2O_3, γ: γ-Al_2O_3 and SN: α-Si_3N_4).
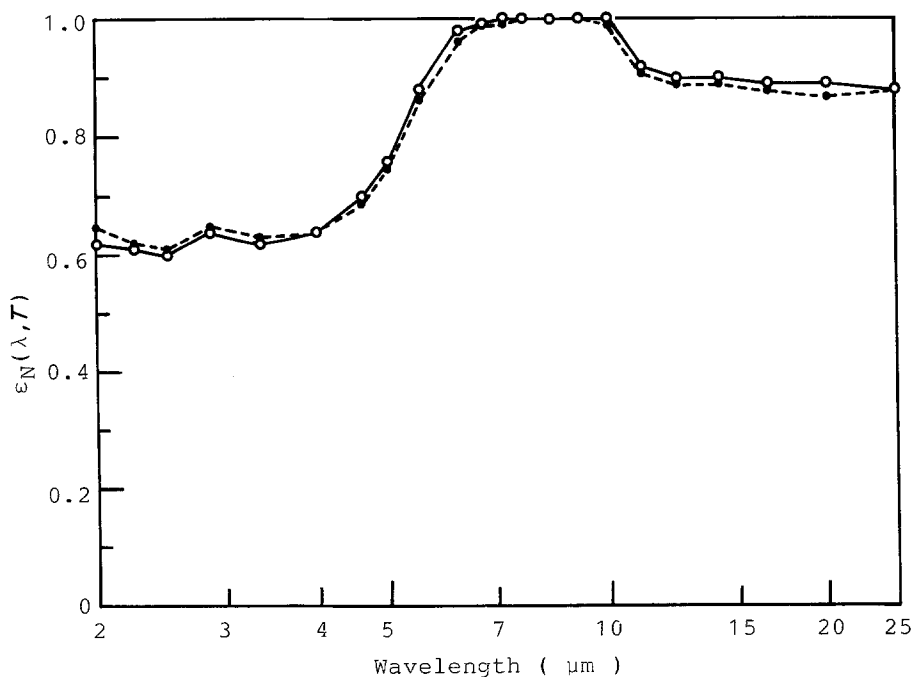
Figure 8 Normal spectral emissivity of Al_2O_3–5.0 wt % Si_3N_4 coating at (●) 795 and (○) 994 K.

$$\int_0^{\lambda_1} M_b(\lambda, T)\, d\lambda = 0.1 M_b(T) \qquad (2)$$

$$\int_{\lambda_2}^{\infty} M_b(\lambda, T)\, d\lambda = 0.1 M_b(T) \qquad (3)$$

where λ is the wavelength, T the temperature, $M_b(\lambda, T)$ the spectral exitance of a black body and $M_b(T)$ the total exitance of a black body. Here we define the region of calculation with λ_1 and λ_2 given by Equations 2 and 3. The calculated $\varepsilon_N(T)$ of Al_2O_3 and Al_2O_3–5% Si_3N_4 coatings at 795 and 944 K are given in Table V. It was found that the $\varepsilon_N(T)$ of the Al_2O_3–5% Si_3N_4 coating decreased with increasing temperature in a similar way to that reported by other researchers for alumina or alumina coatings [11, 12]. In addition, the emissivities found in this work were approximately equal to those obtained on other plasma-sprayed Al_2O_3 coatings.

4. Conclusion

In order to strengthen plasma-sprayed coatings, we have made alumina coatings reinforced by SiC or Si_3N_4 whiskers. As a result, we found that the whisker-reinforced coatings had improved thermal shock resistance, impact toughness and adhesion. Various analytical methods have revealed that the silicon nitride in the Al_2O–Si_3N_4 coating remained as Si_3N_4 whiskers without α–β phase transformation or any reaction between the Si_3N_4 and the Al_2O_3 matrix. The emissivity of the coating was not significantly changed by the incorporation of the whiskers.

References
1. G. F. HURLEY and F. D. GAC, *Amer. Ceram. Soc. Bull.* **58** (1979) 509.
2. E. FITZER, in Proceedings of International Symposium on Factors in Densification and Sintering of Oxide and Non-oxide Ceramics, edited by S. Somiya and S. Saito, (Gakujitsu Bunken Fukyu-kai, Japan, 1979) p. 618.
3. E. T. TURKDOGAN, P. M. BILLS and V. A. TIPPET, *J. Appl. Chem.* **8** (1958) 296.
4. W. A. FORGENG and B. F. DECKER, *Trans. AIME* **212** (1958) 343.
5. S. C. SINGHAL, *Ceramurgia Int.* **2** (1976) 123.
6. K. WEFERS and G. M. BELL, "Oxides and Hydroxides of Aluminium" (Aloca Research Laboratories, 1972).
7. R. McPHERSON, *J. Mater. Sci.* **8** (1973) 851.
8. M. VARDELLE and J. L. BESSON, *Ceram. Int.* **7** (1981) 48.
9. N. N. AULT, *J. Amer. Ceram. Soc.* **40** (1957) 69.
10. C. G. DODD and G. L. GLEN, *ibid.* **53** (1970) 322.
11. A. H. SULLY, E. A. BRANDES and R. B. WATERHOUSE, *Br. J. Appl. Phys.* **3** (1957) 97.
12. A. F. GRENIS and A. P. LEVITT, *Amer. Ceram. Soc. Bull.* **44** (1965) 901.